JOURNAL OF MATERIALS SCIENCE 23 (1988) 1948–1954

Infra-red imaging of current distributions in non-uniform conductive composites of polypropylene filled with stainless steel fibres

B. BRIDGE, M. J. FOLKES*, H. JAHANKHANI*
*Department of Physics, and *Department of Materials Technology, Brunel University, Kingston Lane, Uxbridge, Middlesex UB8 3PH, UK*

The conductivity of bulk samples of polypropylene non-uniformly loaded with 1.2 vol% fraction of stainless steel fibres, has been examined. Local variations in surface temperature caused by non-uniform current flow have been imaged with an infra-red camera. However it was found that there was no simple relationship between the temperature contours and the local fibre density. In particular, the occurrence of small hot spots in two samples did not correlate with fibre concentrations significantly higher or lower than average. Equally, the myriad of tiny, slightly hot or slightly cold spots of ~1 mm dimensions, visible in all the images, did not correlate with fibre-rich or matrix-rich areas. This result is interpreted theoretically by the use of a simple equivalent electric network of the samples, containing twelve identical impedances, corresponding to constant fibre concentrations plus one different impedance which simulates a perturbation in fibre concentration.

1. Introduction

It is easy to underestimate the current interest in polymer-based conductive composites. From a commercial viewpoint their use in practical, cost-effective shielding applications for computer and defence installations is well established. From a more fundamental theoretical standpoint, they serve as potential models of intrinsically conducting polymers and in particular as models of neurological action in living matter. There is now a substantial literature [1–7] on conductive composites, with many of the experimental studies primarily adopting an empirical approach. In view of the number of variables involved, this is probably not an optimum route for developing these materials, even from the purely practical viewpoint of producing high-performance electrical materials for direct industrial applications. We seek a more fundamental evaluation of the physics of the conduction process. To this end we are analysing both the overall levels of volume resistivity and detailed current distributions, in stainless steel fibre-filled polypropylene plaques, as a function of size, shape, orientation and volume fraction of fibres. The basic polymer has a resistivity of $\approx 10^{15}\,\Omega$cm, whereas resistivities of less than $100\,\Omega$cm are readily obtained in samples where the filler volume fraction is sufficiently low that uninterrupted metallic paths between the fibres and electrodes may not exist. It seems possible that conduction in the polymer matrix itself is greatly enhanced by the presence of the metal fibres. Under these conditions several mechanisms are open to consideration; (a) percolation mechanisms as envisaged by McCullough [7], (b) microscopic breakdown across the matrix between nearest neighbour fibres caused by high local electric fields surrounding the small radii of the fibre-tips; (c) treeing phenomena associated with the former; (d) junction effects leading to non-linear phenomena; (e) hopping mechanisms between fibres along polymer chains.

Experimentally, we propose that infra-red thermal imaging provides an interesting first step towards an understanding of the current distributions in composites. At the very least, the temperature distribution within a specimen through which a current is passing could, in principle, distinguish between macroscopically homogeneous current densities and specific conducting paths as conceived by percolation theory.

If j is the current density flowing normally through a vector area, $\mathrm{d}\boldsymbol{A}$ along a normal path, $\mathrm{d}\boldsymbol{r}$, the power dissipation in the volume $\mathrm{d}V = \mathrm{d}\boldsymbol{A}\mathrm{d}\boldsymbol{r}$ is $j^2\,\varrho\mathrm{d}\boldsymbol{A}\mathrm{d}\boldsymbol{r} = \{E^2/\varrho\}\mathrm{d}V$, where ϱ is the resistivity of the volume element and E is the electric field strength within the element (parallel to $\mathrm{d}\boldsymbol{r}$). To a first approximation, the temperature contours imaged by an infrared camera will be in one-to-one correspondence with the local variations in the power dissipation i.e. to variations in $j^2\,\varrho$ (per unit volume) or E^2/ϱ (per unit volume). In fact, local variations in thermal conductivity and convection will complicate the relationship between the power distribution and the surface temperature distribution monitored by the camera. At the same time, one should note that E and ϱ, and j and ϱ are, in fact, interdependent, making the quantitative relationship between surface temperature distribution and current distribution difficult to assess.

2. Sample preparation

For our purposes a batch of composites in the form

0022–2461/88 $03.00 + .12

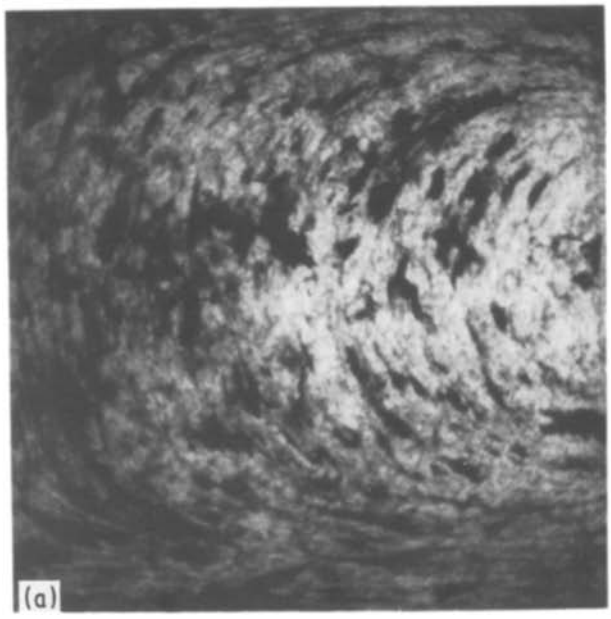

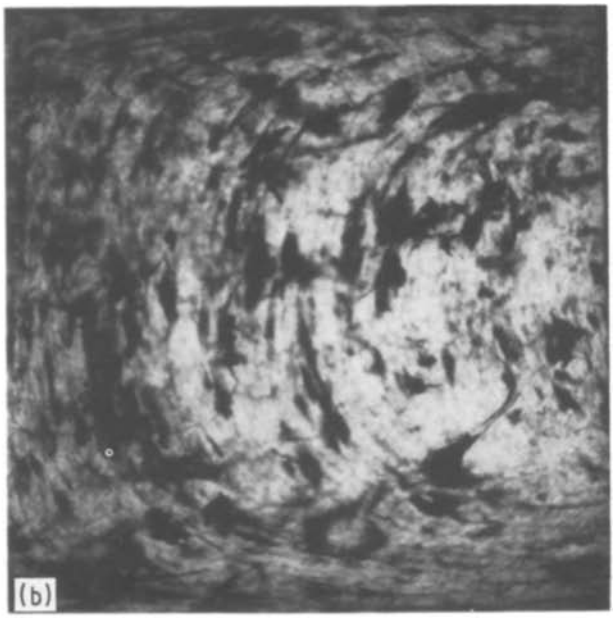

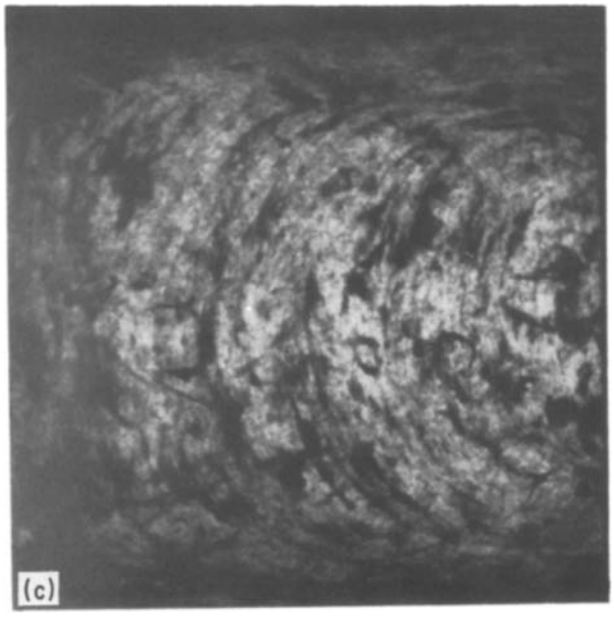

Figure 1 Fibre distribution in the samples, poor dispersion being deliberately engineered to examine the effect on infrared images. The moveable electrodes of the samples holder are connected to the left- and right-hand sides, respectively, as illustrated. (a) Sample A, (b) Sample B, (c) Sample C.

of 80 mm square by 3 mm thick plaques were prepared using a polypropylene resin as the matrix and stainless steel fibres as the filler. The resin, supplied by I.C.I (product code GWM22) was in granular form and had the following properties: density 0.817 g cm^{-3}, melting point 440 K, and an electrical resistivity exceeding 10^{15} Ω cm. The stainless steel fibres, manufactured from 316L grade stainless steel, and supplied by the Bekaert Steel Wire Corporation had lengths in the range 2 to 5 mm, radii of about 4 μm, an electrical resistivity of 74×10^{-6} Ω cm and a density of 7.98 g cm^{-3}. Weighed amounts of polypropylene and stainless steel fibres were thoroughly mixed for 30 min in a rotary blender, using various fibre loadings between 0.2 to 2% volume fraction. These mixtures were injection moulded using a Sandretto Type 6CV/50 microprocessor-controlled injection moulder and a double film-gated mould cavity. After many trials, fibre breakdown was found to be minimized using the following processing conditions: screw speed 80 r.p.m., injection speed 36 cm^3 sec^{-1}, injection pressures 82.5 MPa (first phase), 148.5 MPa (second phase), back pressure, 0.2 MPa, injection time 1.55 sec, mould temperature 40° C, and barrel temperatures of 180, 200, and 240° C, in zones 1, 2, and 3, respectively. Subsequent microscopic examination of some 200 fibres revealed that the mean fibre length in the plaques prepared under these conditions was 800 μm and hence the aspect ratio was about 100.

3. Experimental procedure

For our preliminary experiments it was actually advantageous to examine samples with poor particle dispersion and we selected three samples like this (A, B, and C) which had approximately the same volume fraction of filler (1.2%) but with different fibre dispersions. The weights of these samples (17 g) confirmed the volume fraction of fibres. The macroscopic fibre dispersions can be seen in Fig. 1 which are photographs of optical slide projections of the three samples under very strong light. For the electrical measurements the edges of the mouldings were milled so that they contained surface-breaking fibres round all edges. This process reduced the samples' sides to a uniform length of 79 mm. Additionally, two parallel edges were coated with silver dag to serve as electrodes. The samples were supported in a perspex holder (Fig. 2), which permitted flat, rigid copper electrodes, lined with an aluminium foil, to contact the two silver-dag-coated sample edges. Contact pressures could be varied by advancing two parallel screws (2BA threads).

For present purposes and conductivity levels, a simple two-terminal electrical network employing simple digital voltage and current meters with respective sensitivities of 10^{-6} V and 10^{-6} A, was perfectly adequate. A stabilized variable power supply (0 to 50 V, 0 to 1 A) was connected in series with the sample electrode connections and the current meter, the

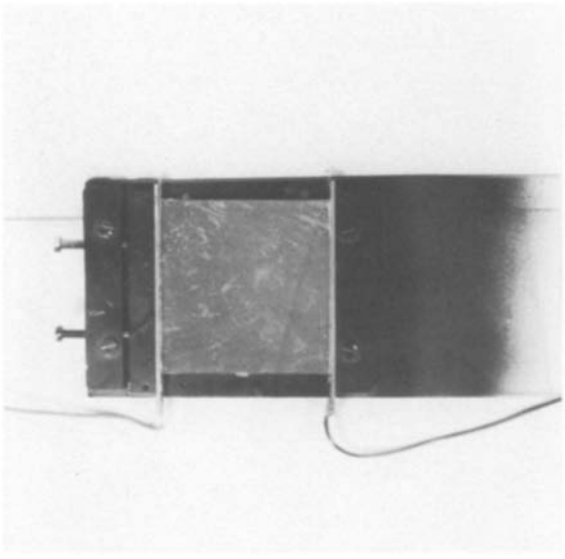

Figure 2 Sample holder.

voltmeter being connected in parallel across the electrodes. From the two meter readings the sample resistance could be measured as a function of applied voltage or sample power dissipation level to study non-linear effects (on simple thermodynamical grounds, conductive composites may be non-ohmic because they constitute a non-uniform system, i.e. they have more than two degrees of freedom). The perspex holder minimized thermal conduction losses from the sample so that the infra-red images obtained were as close as possible to what would be obtained with a thermally isolated sample. The entire holder (excepting the electrodes) was sprayed black to provide a thermally uniform background.

Images were obtained using an AGEMA infra-red system with the camera located 1 m from the vertically sited samples. The images displayed in Figs 3 to 6 are monochrome reproductions from computer print-outs which employed a 16 tone colour scale (black through to pale yellow) spanning a temperature difference of approximately 3.2° C in 0.2° C intervals. Electrical data are included in the figures.

4. Results and discussion

Typical results, together with associated electrical data, are given in Figs 3 to 6, which seek to display the possible effect of fibre dispersion, overall power dissipation level, and contact pressure on the thermal images. In these figures the sample orientations are constant throughout and as shown in Fig. 3, with the electrodes positioned vertically, the moveable electrode being on the right-hand side. The thermal images of the electrodes are just visible as thin vertical lines in some of the figures. The three samples are compared at constant power levels of 5 mW (Figs 3a to c), 10 mW (Figs 4a to c), and 15 mW (Figs 5a to c), respectively, with minimum electrode contact pressure (finger-tight screws) in all cases. In Figs 6a to d the effect of contact pressure on Sample B, at a constant power level of 10 mW, is displayed, the pressure being expressed in terms of sample strain. Careful inspection of these figures yields a number of interesting conclusions.

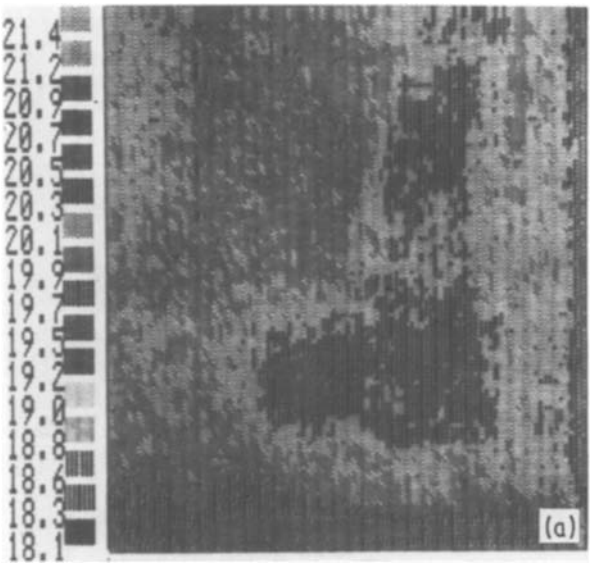

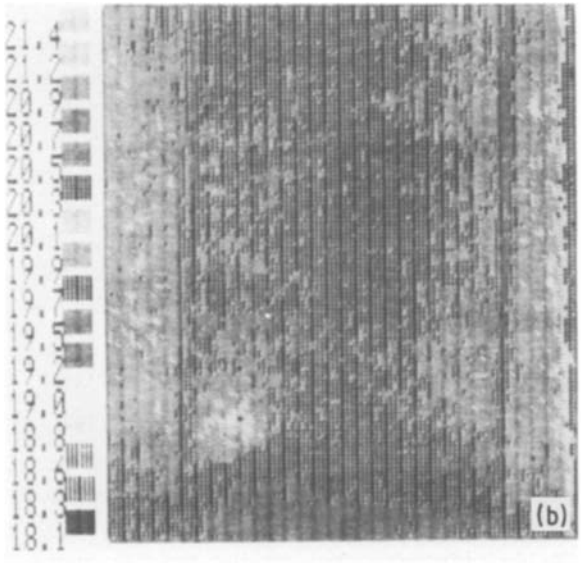

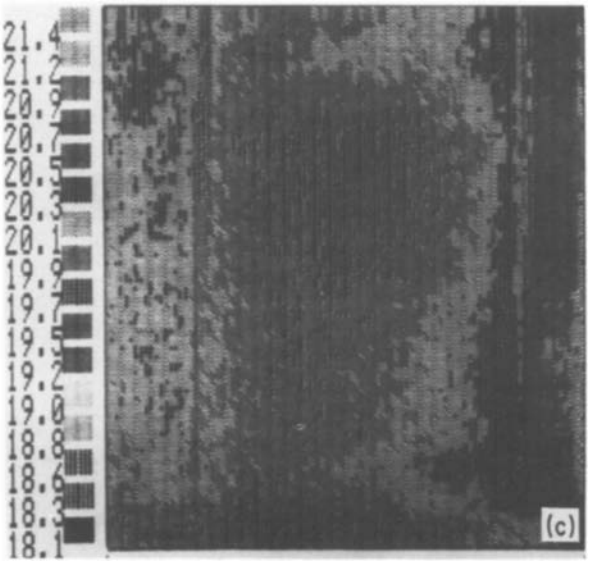

Figure 3 Infrared images of samples after dissipating 5 mW for 5 min. (a) Sample A, 3.57 V, 1.4 mA, ϱ = 775 Ω cm; (b) Sample B, 2.32 V, 2.15 mA, ϱ = 328 Ω cm; (c) Sample C, 1.22 V, 4.1 mA, ϱ = 89 Ω cm.

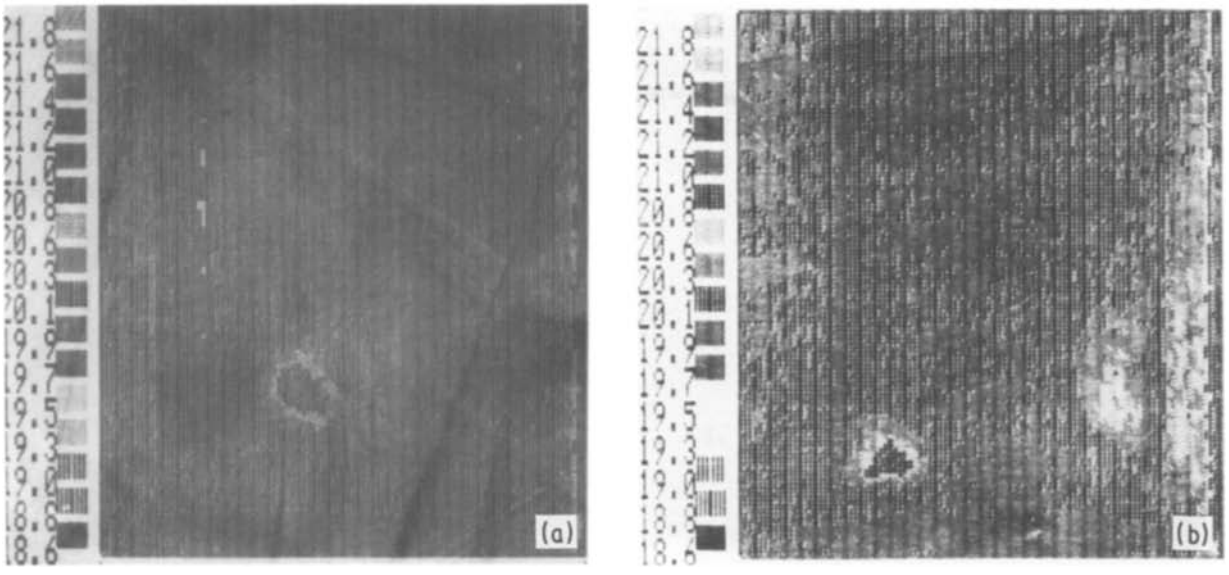

Figure 4 Infrared images of samples after dissipating 10 mW for 5 min. (a) Sample A, 5.0 V, 1.895 mA, $\varrho = 778\,\Omega$cm; (b) Sample B, 3.31 V, 3.0 mA, $\varrho = 335\,\Omega$cm; (c) Sample C, 1.7 V, 5.8 mA, $\varrho = 88\,\Omega$cm.

1. Evidence of non-uniform power distributions caused by inhomogeneous fibre dispersion has been established. We claim this because the change in the surface temperature distribution when comparing Samples A, B, and C at constant power level is more substantial than the differences between the images of any one sample compared at different power levels. This can be seen most easily by considering the strongest features of the temperature distribution of each sample. Sample A has a "hot spot" (about 2° C higher than the mean temperature and 3.5° C higher than the lowest temperature), surrounded by concentric temperature contours, to the bottom left of the image. A similar, though weaker feature, is present in Sample B, located closer to the bottom left-hand corner of the image. Sample C, on the other hand, has a rectangular feature of intermediate temperature, in its temperature contours, to the top right-hand edge of the image. Each of these three features, so different in the three specimens, retain their identity (shape and position) when the power level is changed from 5 to 15 mW, confirming that they are genuine "sample" effects. Finally, also supporting our claim of a fibre-distribution effect in the images, is the behaviour of Sample B under varying contact pressure (Fig. 6). Here we see that the hot spot and surrounding contours remain substantially independent of contact pressure, as does the temperature distribution in the main body of the sample, the contact pressure effect being evident only in the region of the moveable electrode. In fact, thermal imaging also appears to have potential as a method of investigating the quality and nature of electrical contacts.

2. Although fibre dispersion has been proven to affect the temperature distribution, inspection of Fig. 3 (in comparison with Fig. 1) shows that there is no obvious simple relationship between the fibre density and the temperature contours. It is not, for example, possible to associate either high or low fibre concentrations with the hot spots in Samples A and B. More generally, the myriad of tiny, slightly hot or slightly cold spots of only millimetre dimensions, visible in all the images, do not correlate with fibre-rich or matrix-rich areas. This fact, the most interesting result of our study, will be discussed in theoretical terms later.

3. Although variations of sample resistance with contact pressure (at constant power level) were minimal ($\sim 10\%$), pronounced changes in the temperature distribution in the vicinity of the moveable electrode is evident in Figs 6a to d. A region slightly cooler than average appears to grow as the pressure decreases. This is noteworthy, given that increased contact pressure improves the thermal contact between the electrodes (which act as heat sinks) and the sample. There are several possible causes:

(i) The electrical conductivity of the silver dag electrodes could change under compression.

(ii) Fibres, not quite contacting the electrodes in the normal specimen, could be brought into contact with the electrodes, under compression, so reducing local values of resistivity in some regions near the electrodes.

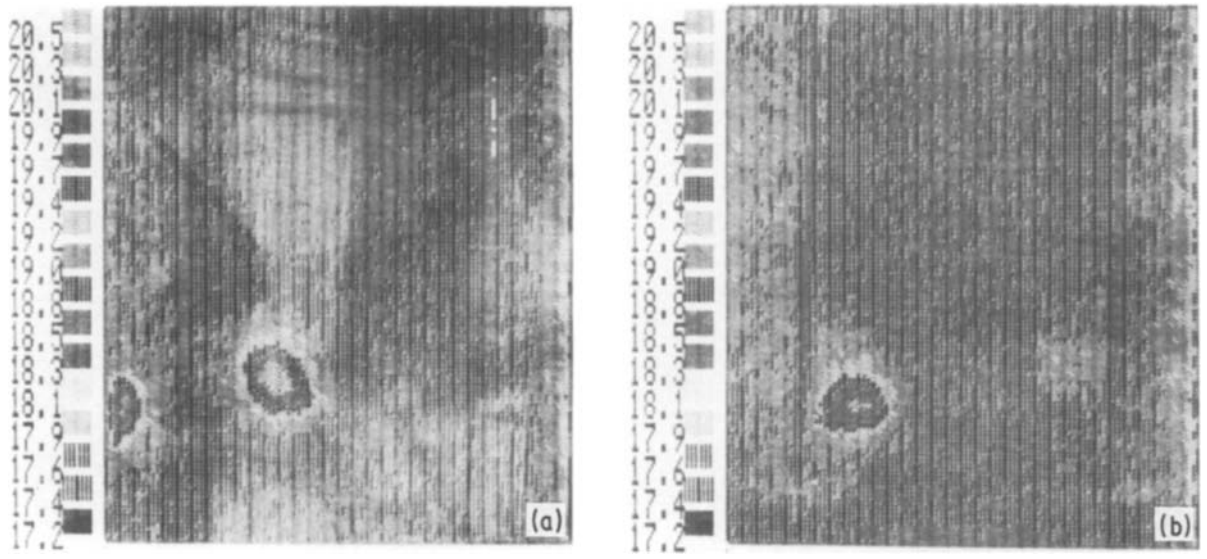

Figure 5 Infrared images of samples after dissipating 15 mW for 5 min, (a) Sample A, 6.25 V, 2.4 mA, $\varrho = 791\,\Omega$cm, (b) Sample B, 3.95 V, 3.8 mA, $\varrho = 315\,\Omega$cm, (c) Sample C, 2.07 V, 7.3 mA, $\varrho = 85\,\Omega$cm.

In this connection it is important to note that fibre–electrode contact is an important determinant of conductivity levels in composites even in specimens lacking internal fibre–fibre contact. If mouldings with unmilled edges are employed, much higher resistivity levels than those reported here are obtained.

(iii) The thermal conductivity of the electrode–sample interface, and in particular the silver dag, is changed under compression. If this mechanism is operative, the temperature distribution round the electrodes may bear a lesser resemblance than otherwise to the current distribution.

All the above effects are restricted to the electrode region and are therefore consistent with the observed insensitivity of the overall resistance of the sample to contact pressure. However, they complicate the attempts to study current distributions by infrared techniques.

The original objective of this paper was to investigate the use of thermal imaging for identifying the conduction mechanism in conducting fibre composites. However, it now appears that the formation of hot spots in the sample dominate the thermal image, at least for the specimens that we have been employing where the fibre dispersion is poor. In fact, the result is of considerable significance commercially, because the moulding technique that we have used in our work is that recommended by moulding companies involved in the fabrication of components for d.c. and electro magnetic interference (EMI) shielding applications. Hence it will be interesting to examine simple possible theoretical models of this most obvious feature of our results, i.e. the "hot spot" in Samples A and B and the fact that high or low fibre concentrations do not seem to correlate with these "hot spots". We represent a rectangular sample of conducting composite with parallel edge electrodes by the network shown in Fig. 5. The resistance $R \neq r$ represents a local non-uniformity (e.g. a variation in fibre volume fraction) in an otherwise uniform sample. In a macroscopically uniform sample ($R = r$) the electric field lines are all parallel to each other and perpendicular to the electrodes, i.e. in Fig. 7 $i_3 = i_1 = i_4$ and the cross currents i_2 are zero. With the local non-uniformity, distortion in the field lines occurs so that transverse current components are possible, i.e the transverse resistances causing finite currents i_2 in the networks. Considerations of symmetry mean that only six different currents are possible in the network; i_1 to i_4, i and I, and application of Kirchoff's laws yields the equations

$$
\begin{aligned}
V &= i_3 2r + i_4 r \\
0 &= i_1 r + i_2 r - i_3 r \\
0 &= IR - i_2 2r - i_4 r \\
i_1 &= 2i_2 + I \\
i_3 &= i_4 - i_2 \\
i &= i_1 + 2i_3
\end{aligned}
$$

where V is the voltage across the electrodes (i.e. between the terminals in Fig. 7).

Elimination of i_1, i_2, i_3 and i_4 yields

$$I = 3V/(4r + 5R), \quad i = I(4R/3r + 5/3)$$

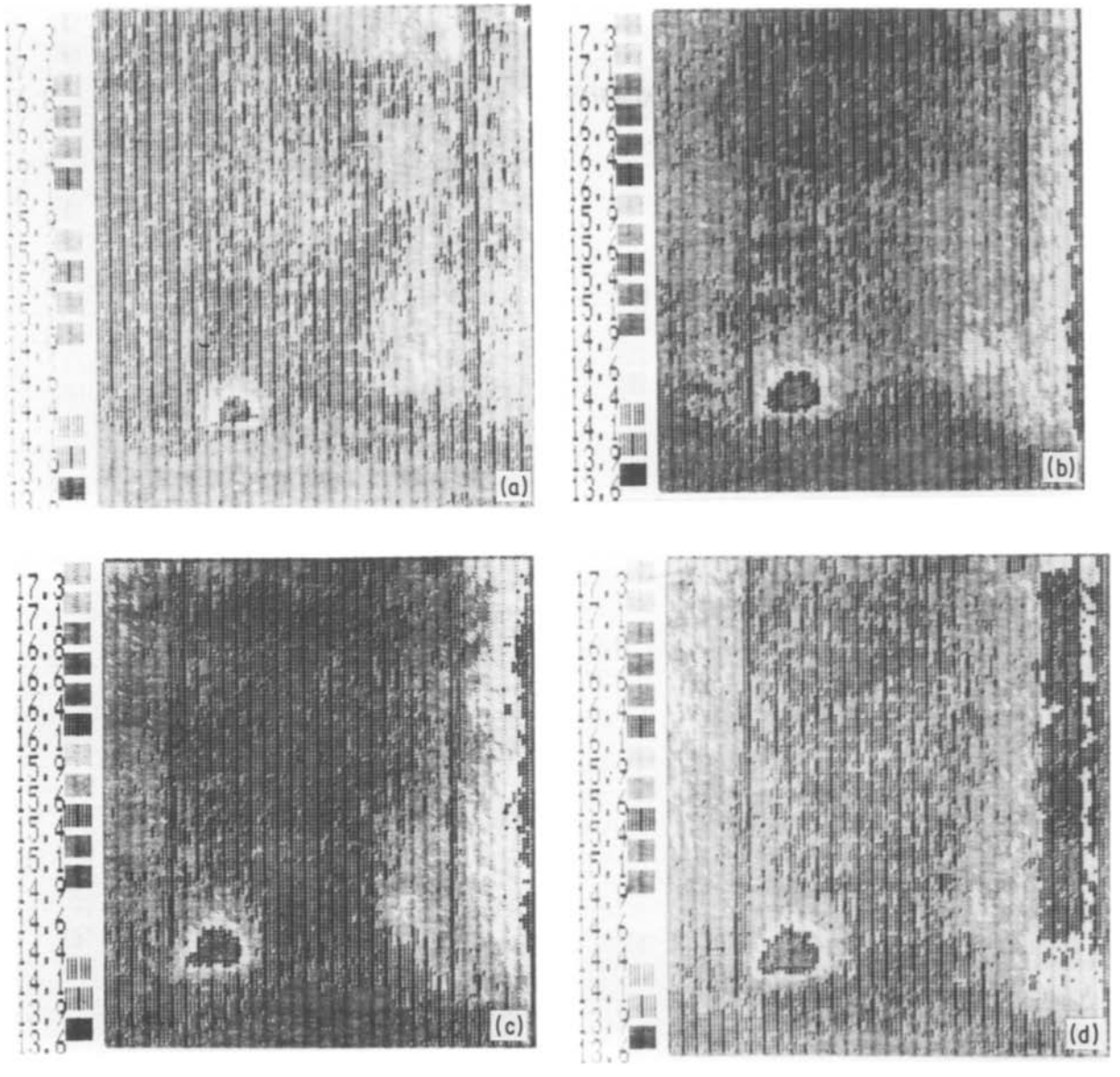

Figure 6 Infrared images of Sample B after dissipating 10 mW for 5 min, with different electrode contact pressures, measured here in terms of the fractional reduction in separation ε of the rigid copper electrodes, (a) $\varepsilon \approx 0$, (b) $\varepsilon = -2 \times 10^{-3}$; (c) $\varepsilon = -4.78 \times 10^{-3}$, (d) $\varepsilon = -6.78 \times 10^{-3}$. The strain in the sample normal to the electrodes is somewhat less than these figures because the sample suffered slight flexure under pressure.

and the ratio of the power dissipation in R to the total power dissipation P is

$$\varrho/P = I^2 R/V = 29Rr/(4r + 5R)(14R + 15r) \quad (1)$$

For $R = r$, $\varrho/P = 1/9$, as would be expected, because i_2 will be zero and equal power flows takes place through the nine longitudinal resistances, with no power flow through the transverse resistances. ϱ/P is in fact a maximum for $R = r$ and becomes zero for both $r/R \to 0$ and ∞. Thus cold spots are to be associated with metal fibre loadings much higher or lower than the normal uniform value. Furthermore local regions of relatively high Joule heating input cannot exist on our network model. Presumably local variations in thermal conductivity must also be taken into account to explain hot spots. If we assume that the thermal conductivity K decreases with decreasing fibre concentration then within the central region, K will decrease as R increases. Now for $r/R > 1$ the Joule heating input (expressed as a fraction ϱ/P) decreases with increasing R. The opposite trends in the heat flow into and out of the region, with R, will cause a temperature maximum for some value of R intermediate between r and ∞. Thus a hot spot can be associated with a metal loading slightly less than the normal uniform value.

As stated earlier, the form of the interdependence between local current flows and resistivity values are not obvious, making the relationship between observed surface temperature contours, and the current distributions of interest to us, difficult to assimilate. The simple network model discussed above throws some light on the problem. In principle, the model can be improved by using a network of finer mesh with more components, because it is always possible to generate a sufficient number of independent simultaneous equations to obtain all currents by computer solution. In the finest possible mesh, the circuit elements would consist of the resistance associated with the gap between two nearest-neighbour fibres. The resistance

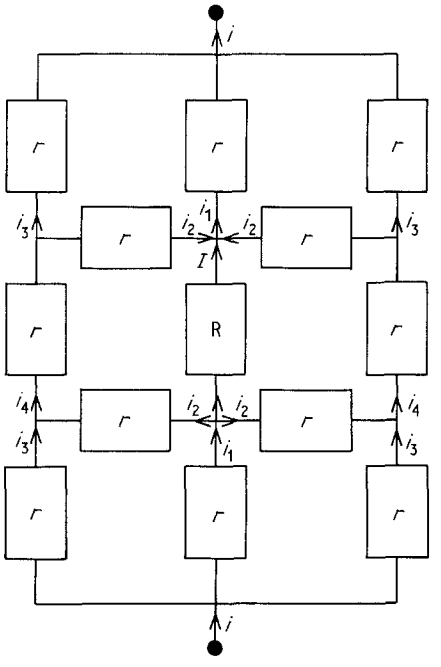

Figure 7 An approximate equivalent d.c. electrical network for a conductive composite in the form of a thin rectangular plate with two electrodes on parallel edges, and of uniform composition apart from a small central region designated by R.

of such elements would be a function of the gap size and fibre orientation, whilst the number of elements having a common junction would depend on the number of nearest neighbour fibres. In this way the network architecture would derive from the distribution and orientation of nearest and next nearest neighbour fibres, and plausibly favourable macroscopic electrical properties may be found to stem from particular macroscopic fibre patterns. Therefore, it is worth noting that a study continues on the electrical properties of basic network elements, consisting of only two drawn fibres embedded in polypropylene, with micrometre scale gaps between the wires and various orientation of the latter. Studies of the thermal image and electrical properties of plaques containing very well dispersed fibres are also underway and the results will be reported in a future publication.

Acknowledgements

The authors thank SERC for financial support for this work, carried out by means of a grant (reference number GR/D/50677) awarded under their specially promoted programme on electroactive polymers. The loan of the infrared imaging apparatus by the SERC Polymer Engineering Directorate is also appreciated. The stainless steel fibres were kindly provided by Bekaert Corporation.

References

1. D. M. BIGG, *Composites* **2** (1979) 95.
2. D. M. BIGG and D. E. STUTZ, *Polym. Compos.* **4** (1983) 40.
3. R. H. WEHRENBERG, *Mater. Engng* **95** (1982) 37.
4. J. W. MORIARTY Jr, Coatings that provide EMI shielding for plastics, 40th Annual Technical Conference, Plastics Meeting, "Challenges of the Future", (ANTEC, California, 10 December, 1982), pp. 600–2.
5. J. J. TOON, National Technical Conference, BAL Harbour, Florida. The Plastics ABCs Polymer Alloy, Blends and Composites, 25 to 27 October (1982) pp. 50–1.
6. R. B. SEYMOUR, (ed.), "Conductive Polymers" (University of Mississippi, Mississippi and Hattiesburg, 1981) p. 237.
7. R. L. McCULLOUGH, *Compos. Sci. Technol.* **22** (1985) 3.

Received 30 September
and accepted 23 December 1986